



ANNUAL
REVIEWS **Further**

Click [here](#) to view this article's online features:

- Download figures as PPT slides
- Navigate linked references
- Download citations
- Explore related articles
- Search keywords

Characteristic Sizes of Life in the Oceans, from Bacteria to Whales*

K.H. Andersen,^{1,2} T. Berge,^{1,3} R.J. Gonçalves,^{1,2,4,5}
M. Hartvig,^{2,6,7} J. Heuschele,^{1,2} S. Hylander,^{2,8}
N.S. Jacobsen,^{1,2} C. Lindemann,² E.A. Martens,^{1,2,9}
A.B. Neuheimer,^{2,6,10} K. Olsson,^{1,2} A. Palacz,²
A.E.F. Prowe,^{1,2,11} J. Sainmont,^{1,2} S.J. Traving,^{1,3}
A.W. Visser,^{1,2} N. Wadhwa,^{1,12} and T. Kiørboe^{1,2}

Annu. Rev. Mar. Sci. 2016. 8:217–41

First published online as a Review in Advance on July 8, 2015

The *Annual Review of Marine Science* is online at marine.annualreviews.org

This article's doi:
10.1146/annurev-marine-122414-034144

Copyright © 2016 by Annual Reviews.
All rights reserved

*Author affiliations can be found in the Acknowledgments section.

Keywords

body size, metabolism, allometric scaling, plankton, mixotrophy, fish, whales

Abstracts

The size of an individual organism is a key trait to characterize its physiology and feeding ecology. Size-based scaling laws may have a limited size range of validity or undergo a transition from one scaling exponent to another at some characteristic size. We collate and review data on size-based scaling laws for resource acquisition, mobility, sensory range, and progeny size for all pelagic marine life, from bacteria to whales. Further, we review and develop simple theoretical arguments for observed scaling laws and the characteristic sizes of a change or breakdown of power laws. We divide life in the ocean into seven major realms based on trophic strategy, physiology, and life history strategy. Such a categorization represents a move away from a taxonomically oriented description toward a trait-based description of life in the oceans. Finally, we discuss life forms that transgress the simple size-based rules and identify unanswered questions.

Power law: $y = bx^a$ with factor b and exponent a ; linear regression employs a logarithmic transformation $\log y = \log b + ax$, with $\log b$ being the intercept and a the slope

Phototroph: an organism that relies on photosynthesis as its carbon source and uses osmotrophic diffusive uptake of nutrients

Mixotroph: an organism that employs a mixed strategy to take up carbon and nutrients, typically combining photosynthesis with phagotrophy

Poikilotherm: an organism that maintains the same body temperature as its environment

Cephalopod: a squid, octopus, or cuttlefish, commonly referred to as inkfish

Cartilaginous fish: fish with skeletons made of cartilage rather than bone; this class (Chondrichthyes) comprises sharks, rays, and skates (Elasmobranchii) as well as ghost sharks (Holocephali)

Homeotherm: an organism that maintains a constant body temperature through internal heat sources

INTRODUCTION

Since Haldane's (1928) essay "On Being the Right Size," biologists have used organism size as a master trait to characterize the capabilities and limitations of individual organisms. There are good reasons for doing so. It is evident that the physiology and ecology of a copepod and a dolphin are vastly different, much more so than those of a copepod and a fish larva. Through power-law functions, organism size can be used to describe aspects of populations and organismal physiology across taxa (Peters 1983), including metabolism (leading to the celebrated 3/4 law for the scaling of resting metabolism with size) (Hemmingsen 1960, Kleiber 1932, West et al. 1997, Winberg 1960); population growth rates (Fenchel 1974, Gillooly et al. 2002); predator-prey relationships in terms of functional response (Hansen et al. 1997, Kiørboe 2011, Rall et al. 2012) and predator:prey size ratios (Barnes et al. 2008, Cohen et al. 1993, Hansen et al. 1994); fluid mechanical forces (Bejan & Marden 2006); swimming speed (Kiørboe 2011, Ware 1978); vision (Dunbrack & Ware 1987); diffusive uptake affinities (Aksnes & Egge 1991, Berg & Purcell 1977, Edwards et al. 2012, Litchman et al. 2007, Munk & Riley 1952, Tambi et al. 2009); and, for phytoplankton, affinities for light (Finkel 2001, Taguchi 1976) and maximum uptake rates (Edwards et al. 2012, Marañón et al. 2013). Size has also been used to describe macroecological patterns of size-dependent species diversity (Fenchel & Finlay 2004, May 1975, Reuman et al. 2014), and the biomass distribution of individuals as a function of size across major taxa (Boudreau & Dickie 1992, Sheldon & Prakash 1972) has been explained theoretically using the size relationships describing individual physiology (Andersen & Beyer 2006, Sheldon et al. 1977).

While developing these size-based relations, the focus has been on determining the exponent (the slope) and the constant (the intercept), with less attention paid to the sizes that limit the range of their validity. Close inspection shows that some power-law relationships change their scaling exponent and/or intercept around some particular size, or even break down altogether beyond a range of validity. For example, the fluid flow around a whale is turbulent, leading to a dominance of inertial forces and a drag force that scales with the length and velocity squared. By contrast, the flow around a unicellular organism is laminar and dominated by viscous forces, with a drag force that scales linearly with velocity and length. Consequently, the scaling of drag force changes at the organism size where there is a transition between viscous and turbulent flow. As an example of a breakdown, consider visual range: The larger an organism's eyes are, the farther it can see. However, there is an upper visual range determined by the sensitivity of the retina (Dunbrack & Ware 1987) as well as a lower limit of eye size determined by the sizes of the visual elements in the retina and the wavelength of light. The scaling law for visual range is therefore valid only within the upper and lower limits. Such changes or breakdowns in scaling laws have consequences for adaptations and strategies of marine organisms. For example, predators so large that they are in the inertial fluid regime develop a streamlined body shape for efficient swimming, and predators smaller than the lower size of an eye cannot rely on vision.

Haldane (1928) concluded that "for every type of animal there is a most convenient size, and a large change in size inevitably carries with it a change of form." Our aim is to determine the sizes where scaling relationships change or break down and to use those characteristic sizes to explain the fundamental differences in the form and function of marine organisms of different sizes. To this end, we build on the large existing literature of empirical size-based scaling relations and their theoretical explanations.

We categorize pelagic life in the ocean based on size in seven general realms: molecular life (viruses), osmo-heterotrophic bacteria, unicellular phototrophs, unicellular mixotrophs and heterotrophs, planktonic multicellular heterotrophs with ontogenetic growth (e.g., copepods), visually foraging poikilotherms (mainly teleosts, cephalopods, and cartilaginous fish), and homeotherms

Table 1 Characteristic sizes of transitions between major realms of life in the ocean

Transition	Size	Notes
Lower size of a cell	0.15 $\mu\text{m} \approx 10^{-15}$ g _C	Limited by cell wall thickness and to a lesser extent genome size (Equation 8)
Osmo-heterotrophs to phototrophs	10^{-14} to 10^{-13} g _C	Transition from diffusion feeding on dissolved organic matter to photosynthesis (Equation 4)
Phototrophs to mixotrophs	10^{-8} g _C	Transition from acquiring inorganic nutrients by diffusion feeding to acquiring nutrients by active feeding (Equation 5)
Mixotrophs to heterotrophs	10^{-7} g _C (10^{-8} to 10^{-5} g _C)	Transition to acquiring carbon and nutrients solely by predation through active feeding (Equation 6)
Unicellular to multicellular organisms	10^{-6} g _C	Development of vascular networks
Copepods to fish	≈ 1 mg _{WW}	Smallest size for a functional camera eye
Fish to cetaceans	≈ 10 kg _{WW}	Smallest size for maintaining a homeothermic metabolism

(cetaceans, but not seals, penguins, or other animals that do not live their entire lives in the pelagic). This categorization of life is a deliberately crude representation of the roughly 200,000 eukaryotic species and the unknown number of archaea and bacteria in the ocean (May & Godfrey 1994), as it is explicitly designed to facilitate an understanding based on size. We describe the life forms in each realm according to their body size and determine characteristic sizes where there is a transition from one realm to another (see **Table 1**). In this manner, we emphasize body size as a fundamental driver of macroecological patterns in the oceans.

We examine five aspects of life where size is a dominant driver: (a) body temperature; (b) resource encounter through predation, diffusive uptake, or photosynthesis; (c) mobility; (d) sensing through chemical and hydromechanical signals, vision, and echolocation; and (e) life history strategy in terms of adult and progeny sizes (**Figure 1**). To this end, we draw on a wide range of theories: diffusion theory, fluid mechanics, optics, metabolic theory, and optimal life history theory. We review established theoretical and empirical scaling laws and establish characteristic sizes where the scaling laws change or break down. These characteristic sizes are used to formulate hypotheses about the dominant strategy for organisms of a given size within the five aspects—e.g., how an organism obtains carbon (through photosynthetic assimilation of inorganic carbon, from dissolved organic matter, or from particulate organic matter) or which senses it employs for prey encounter. We test the hypotheses by collecting data on strategies of individuals as a function of their size. Because our arguments are general in nature, they apply largely to all aquatic life, but our focus is pelagic marine life. The final synthesis is a description of the dominant forms and functions of life in the oceans. This is used to frame a discussion of strategies and life forms that transcend the general size-based patterns and to point toward unanswered questions.

WHAT IS SIZE?

The size of an organism can be characterized by its weight or by its length. The most common weight measures are wet weight, dry weight, and carbon weight; length is typically measured as the largest linear dimension or the equivalent spherical diameter. Depending on the question, one measure may be more appropriate than the other. For example, the flow around an organism is determined by its linear size and shape, not by its weight. Conversely, the bioenergetic budget

Cetacean: a whale, dolphin, or porpoise

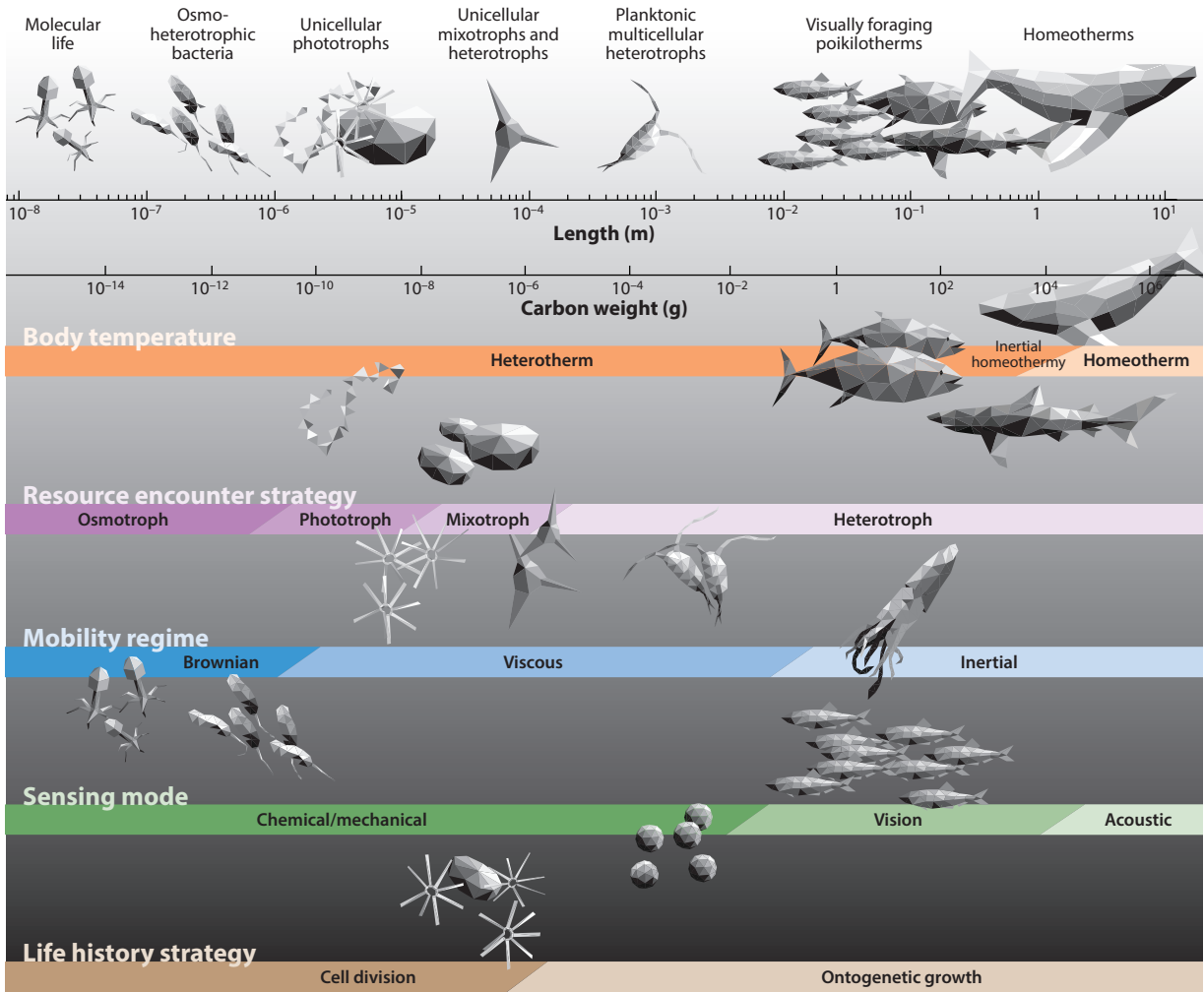



Figure 1

The five aspects of pelagic marine life examined in this review: body temperature, resource encounter strategy, mobility regime, sensing mode, and life history strategy. Each aspect is illustrated in a horizontal bar, with the characteristic transitions indicated by changes in color. The art at the top represents the seven realms of life as defined in this review: molecular life (viruses), osmo-heterotrophic bacteria, unicellular phototrophs, unicellular mixotrophs and heterotrophs, planktonic multicellular heterotrophs (e.g., copepods), visually foraging poikilotherms (mainly teleosts, cephalopods, and cartilaginous fish), and homeotherms (cetaceans).

of an organism is adequately described in terms of weight because the energetic budget should reflect a conservation of mass. For microbes, weight is often measured in carbon or in units of the limiting nutrients because water content and ratios between fundamental elements vary between organisms (Klausmeier et al. 2004). The elemental ratios and water content of vertebrates vary less than they do for invertebrates, so wet weight is often preferred as an intuitive measure of weight for vertebrates. Even though it would be possible to convert all sizes to a common measure, we do not find this useful, and consequently in this review we use the most convenient measure depending on the situation. We use the symbols w for weight, l for length, d for diameter, and r for radius, and we frequently make use of the conversion between length and weight as $w \propto l^3$. Units of weight are

indicated by subscripts, with g_{WW} and g_C referring to wet weight and carbon weight, respectively. Conversion relations are provided in **Supplemental Table 1** (follow the **Supplemental Material link** from the Annual Reviews home page at <http://www.annualreviews.org>).

 Supplemental Material

RESOURCE ENCOUNTER AND TROPHIC STRATEGIES

Organisms acquire carbon and nutrients by feeding on encountered resources, which here refers broadly to dissolved inorganic nutrients, dissolved organic molecules, photons, or prey organisms. Resource encounters occur by three mechanisms: (a) active encounter through cruising, ambushing, or creation of a feeding current; (b) fixation of carbon through photosynthesis; or (c) passive encounter with food items that diffuse toward the feeding individual. The encounter rate (biomass per unit time) is described as

$$E = \beta C, \quad (1)$$

where β is the clearance rate (volume per unit time) and C is the resource concentration (biomass per unit volume). In terms of a type II functional response (Holling 1959), the clearance rate is the slope at the origin, i.e., the potential volume of water cleared for resources per unit time when uptake is not limited by handling time or physiological limits (digestion). These limitations are not considered here. The clearance rate is described as a power function of size $\beta = bl^a$. We employ the linear dimension l to characterize size because resource uptake is determined by the physical size of an organism, not by its weight.

In the following, we describe how the exponent a and the factor b depend on size for the three different resource acquisition mechanisms on the basis of physical processes and empirical cross-species relationships. This analysis allows us to characterize the dominant trophic strategy of particular organisms (e.g., phototrophs or heterotrophs) as a function of their size and the biotic and abiotic environment.

Active Predation

Large protozoans and metazoans have three fundamental modes of actively encountering prey: ambushing, generating a feeding current, and cruising through the water searching for prey (Kiørboe 2011). The clearance rate of each mode (β_A) can be estimated as a velocity multiplied by an encounter cross section. A planktonic filter feeder, for example, captures prey on its filter with a size scaling as the length of the organism squared (l^2), with a feeding-current velocity $u \approx l^{0.8}$ (Huntley & Zhou 2004), leading to a scaling exponent of the clearance rate of $a_A \approx 2 + 0.8 = 2.8$. Similar arguments for the other feeding modes all lead to exponents of approximately 2.8, i.e., slightly below 3, but multiplied by different factors (Kiørboe 2011). Because one feeding mode replaces the other depending on environmental conditions and the size of the prey and the predator, the average life-form-transcending scaling exponent becomes approximately 3 (**Figure 2a**, **Supplemental Table 2**):


$$\beta_A = b_A l^3.$$

Weight-specific uptakes rates, $\propto \beta_A/w$, are therefore independent of size because $w \propto l^3$ (Kiørboe & Hirst 2014).

Photosynthesis

Fixation of dissolved CO_2 by photosynthesis requires encounter with photons (assuming that CO_2 is not limiting). Photosynthesis can in principle occur throughout the cell, but for larger cells it is

Trophic strategy: the strategy used by an organism to gather nourishment; the suffix “-troph” derives from the ancient Greek *trophikós* (τροφικός), meaning “pertaining to food or nourishment”

 Supplemental Material

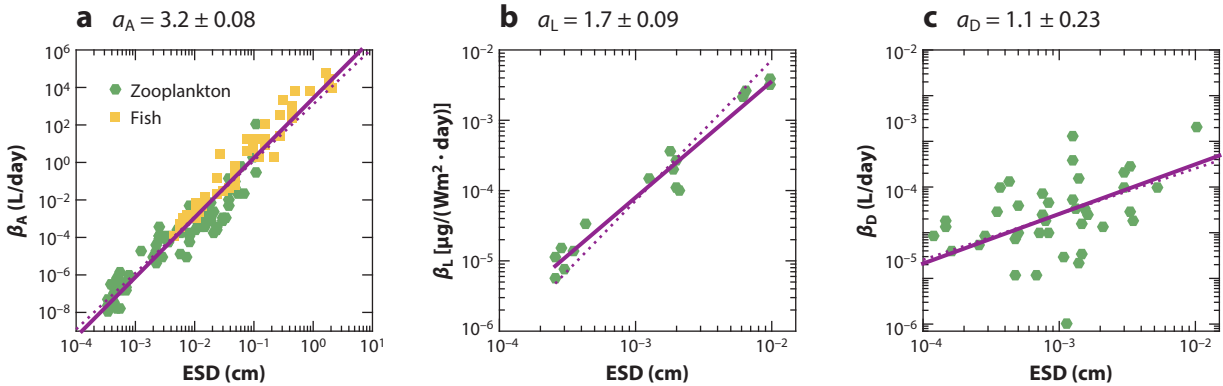


Figure 2

Clearance rate versus weight for organisms performing active predation, photosynthesis, and diffusion feeding on phosphorus. The solid lines are fits to data with the exponent a shown above each panel; the dotted lines are fits with theoretical exponents 3, 2, and 1 for panels a , b , and c , respectively (see **Supplemental Table 2**). (a) Clearance rate β_A for active predation by zooplankton (green hexagons) and fish (yellow squares), from Kjørboe (2011). (b) Clearance rate β_L (affinity) for carbon uptake from a series of experiments with diatoms under identical conditions (Taguchi 1976). Data compilations covering a wider range of sizes and phytoplankton groups give a similar exponent but a larger scatter (Schwaderer et al. 2011). (c) Clearance rate β_D (affinity) for diffusion feeding on dissolved phosphate, from Edwards et al. (2012) and Tambi et al. (2009). Abbreviation: ESD, equivalent spherical diameter.

Supplemental Material

limited by self-shading of photons (the so-called package effect) (Morel & Bricaud 1981). For the present arguments, it is sufficient to consider that the cross-sectional area of the cell $\propto l^2$ limits photosynthesis (**Figure 2b**):

$$\beta_L = b_L l^2. \tag{2}$$

The clearance rate β_L is often termed light affinity or photosynthetic efficiency and is measured in dimensions of carbon fixed per photon multiplied by area. In terms of weight-specific scaling, the power 2 scaling of β_L results in a scaling of weight-specific rates of carbon fixation $\beta_L/w \propto w^{-1/3}$ —i.e., smaller organisms have a higher specific rate of carbon fixation than larger ones. Organisms smaller than a certain size are therefore able to fix more carbon by photosynthesis than by active encounter because specific uptake by active encounter is independent of size.

Diffusion Feeding

Organisms that encounter resource items as they bump into the surface of the organism because of Brownian motion are termed diffusion feeders (Fenchel 1984). Diffusion feeding is used to assimilate dissolved organic molecules, inorganic carbon, and nutrients. The uptake rate is limited by the number of uptake sites on the surface of the cell, which can be expected to scale with l^2 . However, the uptake also removes resources from the vicinity of the cell surface and creates a boundary layer of lower resource concentrations near the cell (Munk & Riley 1952). This effectively leads to the clearance rate β_D being limited by diffusion rather than by the surface, with a scaling proportional to the linear dimension of the cell (reviewed in Fiksen et al. 2013):

$$\beta_D = b_D l^1. \tag{3}$$

Weight-specific uptake rates are then $\propto w^{-2/3}$, i.e., high for small cells and declining with size. Small diffusion-feeding cells therefore have a higher encounter rate with dissolved nutrients or macromolecules than they could have obtained by active feeding. The theoretical scaling

prediction fits with data for phosphate affinity (**Figure 2c**) (p value for a_D different from zero is 2.2×10^{-5}). Data for nitrogen affinity are less clear, with some being consistent with the theoretical scaling ($a_D = 1.2$) (Litchman et al. 2007) and others not ($a_D = 2.25$) (Edwards et al. 2012).

Protists: simple, typically unicellular, eukaryotic organisms that live in aquatic environments

Trophic Strategies

An organism's trophic strategy, i.e., which type of food it consumes, is to a large degree determined by its resource acquisition mechanism. It can be an osmo-heterotroph that diffusion feeds on dissolved organic matter (bacteria), a phototroph that captures light and diffusion feeds on dissolved inorganic nutrients (phytoplankton), a mixotroph that captures light and feeds on other organisms, or an actively feeding heterotroph (animals and many protists). If we use clearance rate as a proxy for competitive ability at low resource concentrations, we can assume that the dominant trophic strategy of organisms at a given size is determined by the resource acquisition mechanism yielding the highest encounter rate. Equation 1 gives the encounter rates for the four trophic strategies as a function of size, where the resource may be concentrations of dissolved organic molecules (C_{DOM}), nutrients (C_N), other prey organisms (C_P), or light flux (C_L). Phototrophs need special treatment because they assimilate inorganic carbon and nutrients by two different processes: Carbon is assimilated through photosynthesis and combined with diffusively encountered nutrients to achieve a C:N ratio c_{CN} . The limiting compound determines the encounter rate as described by Liebig's law of the minimum:

$$E = \min\{c_{CN} \times \beta_D \times C_N, \beta_L \times C_L\}.$$

For a particular environment of light, nutrients, organic matter, and prey, an organism encounters different amounts of resources from the various encounter mechanisms (**Figure 3**). The smallest organisms get the highest encounter rate from diffusive encounter with dissolved organic matter. Diffusion-feeding heterotrophic bacteria (osmo-heterotrophs) therefore dominate among the smallest organisms. As size increases, the encounter rate with photons becomes sufficiently high that photosynthesis combined with diffusive uptake of inorganic nutrients becomes optimal—i.e., the dominant strategy becomes phototrophy. The transition size is when carbon fixation by photosynthesis ($\beta_L C_L = b_L l^2 C_L$) becomes equal to the diffusive encounter with dissolved organic matter ($\beta_D C_{DOM} = b_D l C_{DOM}$), which occurs at a size

$$l = \frac{C_{DOM} b_D}{C_L b_L}. \quad (4)$$

Cells larger than this size are expected to be light-limited phototrophs. When the cells reach a size

$$l = \frac{c_{CN} C_N b_D}{C_L b_L}, \quad (5)$$

the diffusive uptake of inorganic nutrients becomes limiting (Mei et al. 2009). Larger cells still benefit from acquisition of carbon through the aid of photosynthesis, but they are nutrient limited. At a size

$$l = \frac{c_{CN} C_N b_D}{C_F b_A}, \quad (6)$$

active encounter with prey organisms provides the highest encounter rates—i.e., the dominant strategy becomes heterotrophy. There is also a particular size range at which photosynthesis provides more carbon than active encounter (predation) but active encounter provides more nutrients than diffusive uptake of inorganic nutrients. In this range, a mixotrophic strategy is profitable, i.e., using photosynthesis (either from an ingested chloroplast or the organism's own chloroplast)

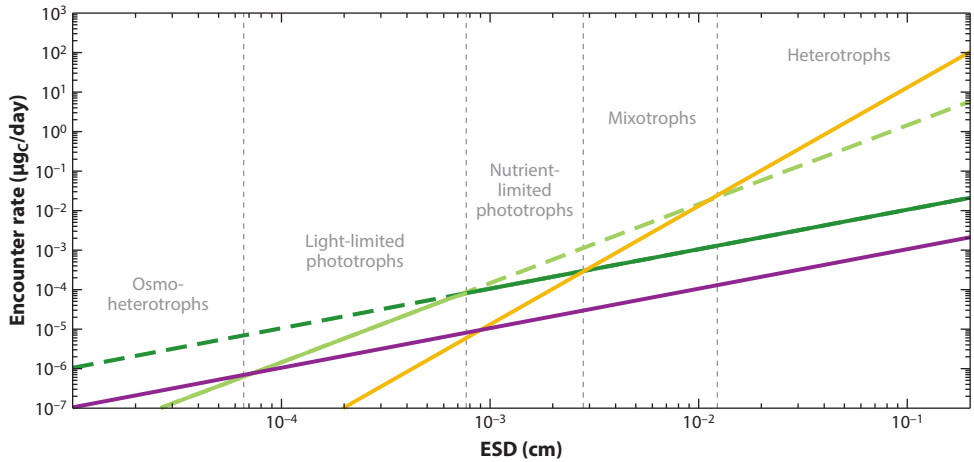


Figure 3

Encounter rates as a function of size for four different resource acquisition mechanisms and resource types: diffusive uptake of dissolved organic matter, scaling as l^1 (solid purple line); uptake of carbon through photosynthesis, scaling as l^2 (dashed light green line); diffusive uptake of dissolved inorganic nutrients (dashed dark green line); and active encounter of prey organisms, scaling as l^3 (solid yellow line). The combined uptake of carbon and nutrients by phototrophs is limited by Liebig's law and shown with solid green lines; light green is used for light-limited conditions, and dark green is used for nutrient-limited conditions. The concentration of dissolved organic matter is $C_{\text{DOM}} = 5 \mu\text{gC/L}$, the concentration of inorganic nutrients is $C_{\text{N}} = 4 \mu\text{molN/L}$ (corresponding to $50 \mu\text{gC/L}$), the light intensity at depth is $C_{\text{L}} = 2 \text{ W/m}^2$, and the concentration of suitable prey organisms is $C_{\text{P}} = 10 \mu\text{gC/L}$. Abbreviation: ESD, equivalent spherical diameter.

predominantly to provide carbon for metabolism, and using active feeding to assimilate nutrients and carbon for biomass synthesis (mixotrophs of types II and III; Stoecker 1998).

The size range in which a certain trophic strategy gives the highest yield depends on the concentration of available resources. If, for example, the concentration of prey organisms increases, the lower size limit where active feeding gives the highest yield decreases. The transition size between the dominant feeding strategies is therefore different under oligotrophic conditions (high light and low nutrient concentrations, such as summer surface conditions in seasonal environments or oceanic regions) than under eutrophic conditions (low light and high nutrient concentrations, such as spring surface conditions in seasonal environments or conditions at depth) (Figure 4a,b). The general pattern of small diffusion feeders, medium phototrophs, and large active feeders is identical between oligotrophic and eutrophic environments, but the sizes at which the transitions occur vary: Oligotrophic conditions give rise to smaller phototrophs and a large size range of mixotrophs, whereas eutrophic conditions lead to larger osmo-heterotrophic bacteria, phototrophs, and mixotrophs. The general pattern fits well with the classical interpretation of the seasonal succession of cell size in temperate systems (Kiørboe 1993): Large cells (diatoms) dominate during nutrient-rich spring conditions but are overtaken by smaller cells (dinoflagellates and cryptophytes), often with a mixotrophic strategy, during the nutrient-depleted summer conditions (Barton et al. 2013).

A compilation of the dominant trophic strategies according to size largely confirms the theoretical predictions while also highlighting the large overlap in the size range between phototrophs, mixotrophs, and small heterotrophs (Figure 4c). The overlap reflects that the compilation is based on observations from various environmental conditions, which, as demonstrated above, create a

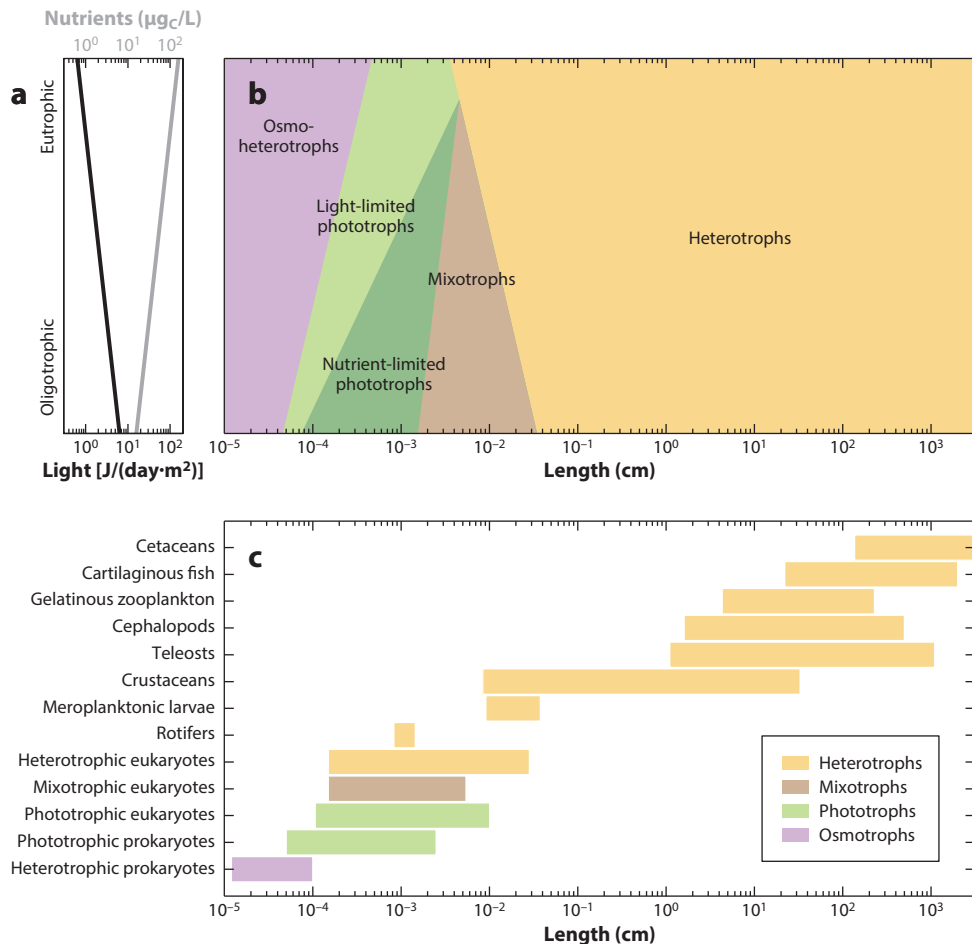


Figure 4

Trophic strategy as a function of size. (a) Resource conditions [nutrients (*gray line*) and light (*black line*)] used to create environments moving from oligotrophic conditions (high light, low nutrients; *bottom*) to eutrophic conditions (low light, high nutrients; *top*). (b) Strategies that yield the highest resource encounter rates as a function of size (*x axis*) and resource conditions (*y axis*). (c) Trophic strategies of 3,020 marine organisms as a function of length. Ciliates and flagellates have been categorized as phototrophs, mixotrophs, or heterotrophs depending on the trophic strategy for the specific species (see **Supplemental Table 3**). The groupings comprise cetaceans (whales, dolphins, and porpoises), cartilaginous fish (Elasmobranchii and Holocephali), gelatinous zooplankton (Cnidaria and Ctenophora), cephalopods (Cephalopoda), teleosts (Osteichthyes), crustaceans (including copepods), meroplanktonic larvae (planktonic larvae whose adult stages are benthic), rotifers (Rotifera), and unicellular eukaryotes or prokaryotes.

significant variation in the transition sizes where one trophic strategy gives a higher yield than another strategy.

MOBILITY

Movement is powered by muscles or flagella and is constrained by friction from the water. From an organism's perspective, the nature of water changes dramatically with size: Large organisms use

[▶ Supplemental Material](#)

their inertia to coast through water, whereas smaller organisms experience water as thick and sticky. Very small organisms have to cope with the random forces of molecules that induce Brownian motion (Dusenbery 2009). The hydromechanics of movement can therefore be divided into three regimes: an inertial regime, a viscous regime, and a Brownian regime. Here, we are concerned mainly with the differences between the inertial and viscous regimes. The hydrodynamic regime determines the forces on the body, which in turn influences the optimal shape. In the viscous regime, the dominating force is surface friction, which scales with the linear dimensions of the body. In this regime, it is therefore optimal to reduce the surface area, i.e., to be spherical (although actually the optimal shape deviates slightly from spherical; Dusenbery 2009). In the inertial regime, the drag force is proportional to the projected frontal area of the organisms, making it optimal to reduce this area by streamlining.

Whether an organism is in the inertial or viscous regime depends on the Reynolds number, $Re = ul/\nu$, which describes the ratio between inertial and viscous forces operating on a body of size l moving at velocity u through water with a kinematic viscosity $\nu \approx 10^{-2}$ cm²/s. The crossover between the two regimes is at $Re \approx 20$ – 30 (Webb 1988). The scaling of swimming velocity with size differs in the two regimes: In the viscous regime, the velocity was found empirically to scale as $l^{0.79}$ (Kiørboe 2011), whereas in the inertial regime, theoretical arguments predict it to scale as $l^{0.42}$ (Ware 1978) or $l^{0.5}$ (Bejan & Marden 2006); observation suggests a scaling $u \propto l^{0.45}$ (Figure 5a). The empirical data indicate a crossover size between the viscous and inertial regimes at a body length of approximately 7 cm, corresponding to a Reynolds number on the order of 1,000. The relevance of size for body shape is evident (Figure 5b): Small organisms do not appear to be constrained in their body shape, whereas fish and mammals are streamlined, with an average aspect ratio of approximately 0.25. Copepods are in between and have a significantly larger aspect ratio than fish. During jumps, however, the Reynolds number becomes large, thus giving them the advantage of a relatively slender body plan (Kiørboe et al. 2010).

SIZE AND SENSING

Actively feeding organisms perceive their prey by chemical or hydromechanical cues, vision, or echolocation. The range of sensing is determined by the size of the predator and the prey; a blue whale with an eye diameter of 15 cm sees much farther than a fish larva with an eye diameter of 1 mm. The sense with the furthest range for organisms of a given size can be expected to dominate among organisms of that size. Organisms using more than one sense complicate the analysis of senses. For example, sharks use smell to follow the trail of a prey at great distances; when closing in on the prey, vision becomes important (Hueter et al. 2004); and at distances below 1 m, they use electro-sensing to precisely locate the prey (Collin & Whitehead 2004). Copepods are generally considered mechanosensing organisms, yet they can sense and follow the chemical trail of a settling marine snow particle (Kiørboe 2001) and the pheromone trail of a potential mate (Bagøien & Kiørboe 2005). Leaving such complications aside, we review estimates of the sensory ranges of four senses where the range depends on the size of the predator: chemical sensing, sensing of hydromechanical signals, vision, and echolocation.

Chemosensing

In that all organisms depend on chemistry in one way or another, it may be safely assumed that they have machinery for chemical sensing. The question is how chemosensing together with behavior can bring organisms into contact with remote resources. The way organisms experience the coherence of chemical gradients and trails is determined by individual size in relation to

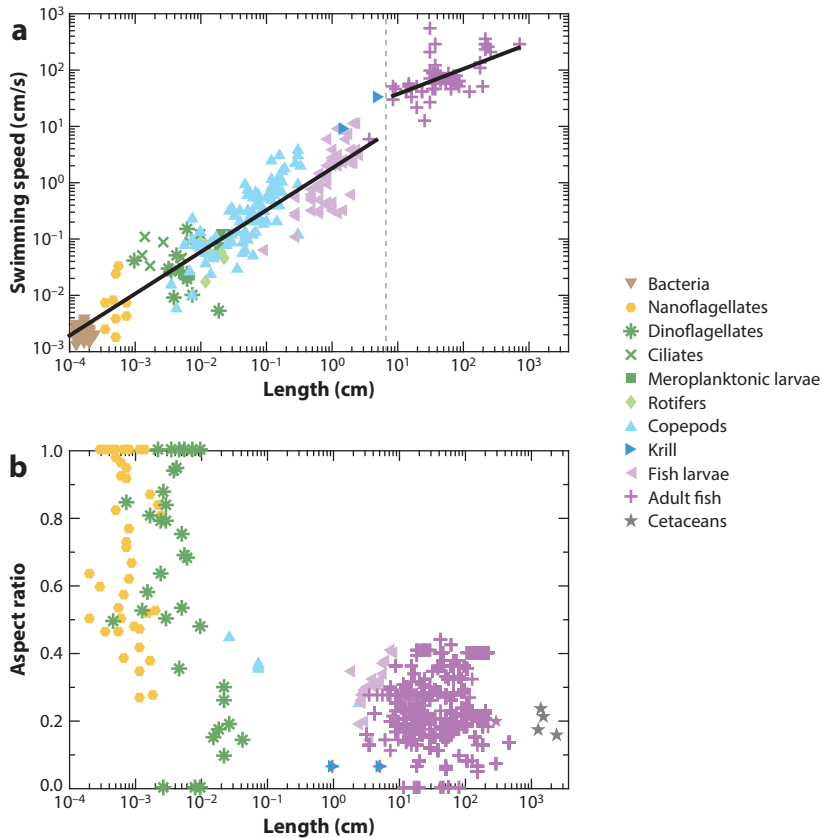


Figure 5

Swimming speeds and body aspect ratio versus body length. Length is measured as equivalent spherical diameter for planktonic organisms and as longest length for krill (*dark blue*), fish larvae (*light purple*), adult fish (*dark purple*), and cetaceans (*gray*). (*a*) Swimming speed as a function of length. Data for zooplankton (including fish larvae) are from Kiørboe (2011); data for fish (cruising speed) are from Sambilya (1990). The lines are power-law fits (see **Supplemental Table 1**). The split between the two data sets was determined as the size that gave the lowest total residual of the fits. The crossover size at 6.6 cm corresponds to a Reynolds number of approximately 1,000. (*b*) Aspect ratio as a function of length for mobile marine organisms. Data for nanoflagellates and dinoflagellates are from Throndsen et al. (2003) and Tomas (1997); data for copepods are from Kiørboe et al. (2010); data for krill are from Watkins & Brierley (2002); data for fish larvae are from Ara et al. (2013), Morioka et al. (2013), Moser et al. (1986), and Oka & Higashiji (2012); and data for adult fish are from Froese & Pauly (2013).

[▶ Supplemental Material](#)

turbulent eddies. Turbulence is characterized by three length scales (Tennekes & Lumley 1972): the Batchelor scale ($\approx 10 \mu\text{m}$ in the upper ocean, where turbulence starts to erode the regularity of a gradient), the Kolmogorov scale ($\approx 1,000 \mu\text{m}$, where turbulence starts to impede the organism's ability to maintain direction), and the integral scale ($\approx 1\text{--}10 \text{ m}$, where turbulent energy is injected by large-scale motions).

We distinguish between two modes of chemosensing: gradient climbing (e.g., bacterial run-tumble) and trail following (e.g., a shark following a prey trail). Gradient climbing relies on a chemical gradient set up by molecular diffusion of a solute from a source. The regularity of such gradients would be scale independent if it were not for turbulence. We can place an upper

Stresslet: a Stokes flow produced by two colinear antiparallel point forces acting on a fluid

boundary for gradient climbing between the Batchelor scale and the Kolmogorov scale, in the range of 10–1,000 μm . Another limitation of the ability to follow gradients created by molecular diffusion is whether the trail is diffusing faster than the movement of the prey. This criterion sets an upper limit for predator size of 50 μm (Kiørboe 2011). For trail following, additional criteria come into effect: the movement of the target organism, the rate at which it releases solute, and how well the searching organism can detect this solute above background levels. In any case, organisms smaller than the energy-containing turbulent eddies will experience the trail as patchy and therefore need to search large areas relative to their own size to follow the trail. This scenario is relevant for organisms of a size between the Kolmogorov and integral length scales, i.e., organisms smaller than 1 m. Organisms larger than the integral scale are able to integrate over the subscale trail details and follow a trail without detours. Trail following is therefore most advantageous for large organisms and/or in quiescent environments, e.g., the deep oceans (Martens et al. 2015).

Mechanosensing

Ambush feeders may sense their prey via the fluid mechanical disturbance created by a moving prey (reviewed in Kiørboe 2011). To enhance the sensory range, they employ special sensory arrangements protruding from the body, like the long seta-studded antennules on copepods or the sensory hairs arranged along the slender bodies of chaetognaths (arrow worms). The fluid mechanical disturbance of a self-propelling prey can be modeled as a stresslet, which implies that the signal attenuates as the cube of the distance away from the prey (Visser 2001). The range at which this signal can be sensed is $R \approx (3l_{\text{prey}}^2 l_{\text{sensor}} u_{\text{prey}} / u^*)^{1/3}$, where u^* is the detection limit of the velocity disturbance and l_{sensor} is the length of the sensor (approximately the size of the predator). For $u_{\text{prey}} = bl_{\text{prey}}^{0.74}$ and a predator:prey length ratio $B \approx 10$, the sensing distance is $R \approx cl^{1.24}$, with $c \approx 1.4 \text{ cm}^{-0.24}$ for $u^* = 33 \mu\text{m/s}$ (Kiørboe 2011) (**Figure 6**). An upper range comes into effect when the turbulent shear γ across the body of the predator organism approaches the sensitivity, i.e., when $u^* = \gamma l$. For moderate turbulent shears found in the upper ocean (0.03 s^{-1} , which is in the middle of the typical range of 10^{-4} – 10^{-1} s^{-1} ; Visser & Jackson 2004), this happens for l in the range 500–1,000 μm . Mechanosensing is therefore most advantageous for small organisms ($<1 \text{ cm}$) or on short ranges for large organisms.

Vision

Eyes contain photoreceptors that detect light and convert it into neuronal signals. The simple eyes of some microorganisms are only able to detect changes in the ambient light sufficient to detect diurnal rhythms, orientation toward the surface, and nearby movement. Active visual predation requires an eye with sufficient resolution to form an image and preferably also active optical machinery to focus a targeted object. With regard to feeding, the most important property of the eye is the distance at which it can discern a suitable prey.

Dunbrack & Ware (1987) modeled the optical and sensing abilities of a camera eye to estimate the visual range of a predator of length l searching for prey with a fixed fraction of the predator size (see sidebar The Dunbrack & Ware Model of Visual Range). Two important conclusions emerge from their arguments. First, the sensing range scales as $l^{1.75}$ in clear water under high light conditions. Second, the maximum range of large organisms is limited by the optical properties of the water. Under perfect conditions, the range is 40–70 m (Davies-Colley & Smith 1995). The range decreases with the ambient light such that at depth, where the inherent contrast is low, visual range is limited mainly by the optical properties of the water.

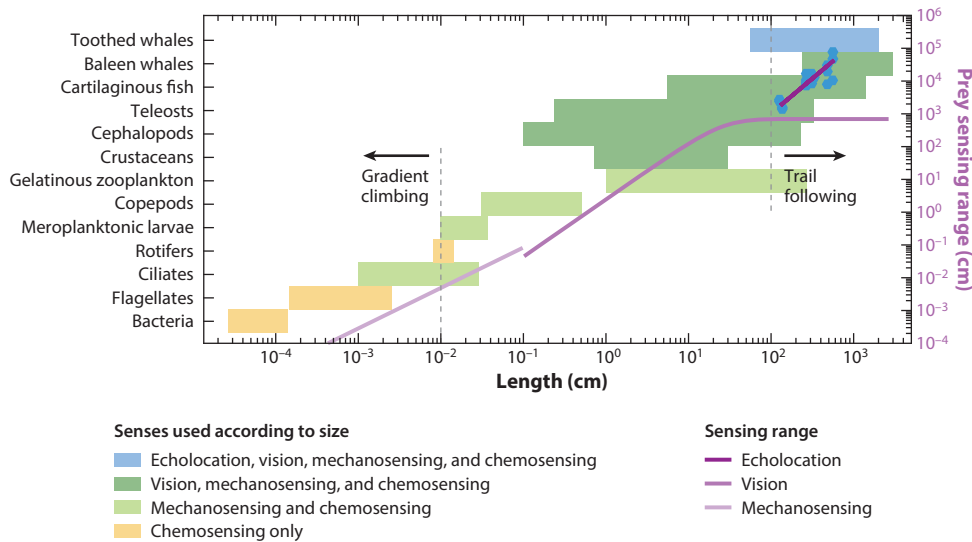


Figure 6

Senses versus size. The left axis and bars show senses used for detecting prey grouped according to size and organismal group (see **Supplemental Table 4**). The right axis and purple lines show the estimated ranges for sensing a prey a factor of 10 shorter than a predator (for details, see sidebar *The Dunbrack & Ware Model of Visual Range*). For toothed whales (including dolphins), the echolocation ranges were determined from tank and field measurements of individuals of different sizes (*blue hexagons*) (see **Supplemental Table 5**); the line is fitted with exponent 17/8 (see **Supplemental Table 1**). The vertical dashed gray lines are estimates of the limits of chemotaxis strategies.

[▶ Supplemental Material](#)

A lower size limit of a functioning eye is determined by the finite size of the photoreceptor. Photoreceptors' functioning relies on opsin molecules (rhodopsin) stacked in rod cells with a width $d_{rod} \approx 1 \mu\text{m}$ (Curcio et al. 1990). Taking account of the universality of the opsin design for photoreception, we may consider this length a limiting factor for building eyes. Considering a minimal resolution for sufficient image formation of (for example) 100^2 results in a retina size of $d_r \approx 0.1 \text{ mm}$. This is approximately one-tenth the size of the smallest aquatic organisms with camera eyes: larval fish and cephalopods. Therefore, vision is only viable as a mode of sensing prey for predators in the size range of a few millimeters and larger.

Echolocation

Echolocation is an active sensing mode in which the animal emits ultrasonic calls and interprets the environment based on the echoes of these calls. It is common for toothed whales (odontocetes), and although it is also used for orientation, here we focus on echolocation and its role in prey detection.

We can estimate how the range R of echolocation scales with the size of the animal based on three assumptions: (a) The sensitivity of the ear, P_0 , is independent of the size of the animal; (b) the emitted power scales with an exponent p as $P_e \propto w^p \propto l^{3p}$; and (c) the frequency-dependent attenuation of sound in seawater can be ignored because this attenuation is small compared with the conical spread of the sound wave. In free space, the emitted signal spreads as a conic beam, resulting in the attenuation of the signal power as R^{-2} . The power of the reflected signal is $P_r \propto P_e l_{prey}^2 (2R)^{-2}$,

THE DUNBRACK & WARE MODEL OF VISUAL RANGE

The maximum visual range in clear water can be estimated by considering the properties of a pinhole camera eye, as was done in a largely unrecognized work by Dunbrack & Ware (1987). Here, we provide a simplified derivation of their argument that also corrects several minor errors.

The projection of a visual image of a prey on the retina of a predator activates a number of visual elements n proportional to the area of the projected image multiplied by the density of visual elements. Because we are interested in the maximum distance R at which an object can be discerned, we can assume that the distance is large relative to the diameter of the eye such that the curvature of the eye can be ignored. The number of activated visual elements is $n \propto \rho l_{\text{eye}}^2 l_{\text{prey}}^2 R^{-2}$, where ρ is the density of visual elements and l_{eye} is the diameter of the eye. The density of visual elements is a decreasing function of the size of the eye: $\rho \propto l_{\text{eye}}^{-d}$, with $d \approx 0.5$ (Dunbrack & Ware 1987). Assuming that the size of the eye and the preferred size of the prey scale with the length of the predator gives the number of visual elements as $n \propto l^{4-d} R^{-2}$.

The largest distance R at which a predator can discern a prey of size (length) l_{prey} is the distance at which the apparent contrast (the difference between the visual imprint of the prey and the background) of the prey (C_a) equals the contrast threshold that the predator can distinguish (C_t). The apparent contrast of the prey declines away from the inherent contrast $C_0 = 0.3$ as $C_a = C_0 e^{-\alpha R}$, where $\alpha = 0.001 \text{ cm}^{-1}$ is the attenuation of light by the water. The contrast threshold is a declining function of the number of visual elements n involved in discerning the object: $C_t = C_{t,\text{min}} + 1/n$, where $C_{t,\text{min}} = 0.15$ is the minimum contrast threshold for vision, which depends on the ambient light. This semiheuristic relationship is known as Ricco's law (Northmore et al. 1978). The maximum distance at which the prey can be perceived is the point at which the apparent contrast reaches the contrast threshold (i.e., where $C_a = C_t$): $C_0 e^{-\alpha R} = C_{t,\text{min}} + KR^2 l^{d-4}$, where $K = 0.025 \text{ cm}^{1.5}$ is a constant that characterizes the sensitivity of the eye.

It is not possible to isolate R from the expression above. However, two limiting cases can be derived. The clear-water limit is where the visual range is limited by the resolution of the eye, i.e., where $e^{-\alpha R} \approx 1$ and $C_0 \gg C_{t,\text{min}}$: $R \approx \sqrt{C_0/K} l^{2-d/2}$. In this case, the maximum visual range increases with $l^{2-2/d} \approx l^{1.75}$ for $d = 0.5$. The turbid-water limit is when the visual range is limited by the sensitivity (the minimum contrast threshold) of a visual element, when $C_{t,\text{min}} \gg KR^2 l^{d-4}$: $R \approx (\ln C_0 - \ln C_{t,\text{min}})/\alpha$. In this limit, the size of the predator does not play a role, and the minimum contrast threshold essentially limits the visual range. The visual range decreases if the light in the water is limited (higher minimum contrast threshold $C_{t,\text{min}}$) or the turbidity α increases. The prediction of this limit has been the subject of more elaborate models (Aksnes & Utne 1997).

where l_{prey}^2 is the area of the reflecting target and the factor 2 is used because the signal attenuates both as it travels toward the target and when it returns. Inserting the power of the emitted signal and absorbing the factor 2 in the proportionality constant gives $P_r \propto l^{3p} l_{\text{prey}}^2 R^{-2}$. The distance where the strength of the returned signal is just at the sensitivity of the ear, i.e., $P_0 = P_r$, scales as $R \propto P_0^{-1/2} l_{\text{prey}} l^{3p/2}$. If the preferred prey size scales with the size of the predator, i.e., $l_{\text{prey}} \propto l$, then

$$R \propto P_0^{-1/2} l^{1+3p/2}.$$

If the power of the emitted sound follows metabolic scaling, $p = 3/4$, then the exponent becomes $17/8$. This argument provides only the scaling of the sensing range; the factor can be found by fitting to data (**Figure 6**).

Size and Sense

The theoretical arguments outlined above identified three characteristic predator sizes where one sense becomes more efficient than another: (a) 100 μm , which is the upper size limit for gradient climbing; (b) between 1 mm and 1 cm, where there is a transition from hydromechanical sensing to vision; and (c) approximately 1 m, which is the point at which predators are able to realize the upper visible range of up to 80 m in clear water. An extension of the sensory range beyond this length can be achieved only by trail-following chemical tracers or by echolocation.

Analysis of body size and senses used by marine organisms reveals that the number of possible senses available to a predator increases with size (**Figure 6**). Large organisms typically combine several senses for foraging. The lower size limit of vision of approximately 1 cm is clearly borne out; this size indeed corresponds to the smallest size of fish and cephalopod larvae. Some large life forms do not use vision to detect prey, most notably the gelatinous zooplankton, even though they are much larger than 1 cm. From this perspective, the strategy of gelatinous zooplankton is to avoid building a vertebrate body (with its associated high metabolic requirements to utilize the increased sensing range that vision provides) and to instead depend on an inflated body to increase the prey encounter cross section (Kjørboe 2013). Because the superiority of vision declines with ambient light, the relative disadvantage of gelatinous zooplankton compared with fish diminishes in turbid waters and in deep waters (Sørnes & Aksnes 2004).

LIFE HISTORY AND PROGENY SIZE

Though obvious on the individual level, the concept of size becomes ambiguous when applied at the species level because all organisms differ in the sizes of their adults and progeny; even unicellular organisms need to double their size before they can divide. The difference between adult and progeny size is most extreme among the teleosts, where the weight ratio between adults and larvae can be up to 10^8 (for bluefin tuna).

Optimal Life History Theory

The evolution of life history with a pronounced difference between adult and offspring size can be understood from optimal life history theory (Andersen et al. 2008, Christiansen & Fenchel 1979). If we assume (a) a standard metabolic scaling of consumption Aw^n with $n \approx 3/4$ (West et al. 1997), (b) a metabolic scaling of mortality αAw^{n-1} (Andersen & Beyer 2006, Hirst & Kjørboe 2002, Peterson & Wroblewski 1984), and (c) determinate growth, then the lifetime reproductive output R_0 becomes

$$R_0 = \frac{\epsilon}{2\alpha} \left(\frac{W}{w_0} \right)^{1-\alpha}, \quad (7)$$

where W/w_0 is the ratio between the weight at maturation and weight of offspring, ϵ is the efficiency of reproduction, and α is the physiological mortality, which is less than 1 (Andersen et al. 2008) (see sidebar Life History Optimization of Offspring Size). Because the exponent $1 - \alpha$ is positive, R_0 is an increasing function of W/w_0 . The metabolic assumptions thus predict an evolutionary pressure toward a life history with as large a ratio as possible between adult size and offspring size. Because no organism has an infinite ratio between adult size and offspring size, a full understanding of what limits actual offspring size cannot be achieved from optimal life history theory based on metabolic scaling laws alone; the actual offspring size will be limited by other processes.

Physiological mortality: the ratio between mortality and weight-specific consumption; with metabolic scaling of uptake $Aw^{3/4}$ and mortality $\alpha w^{-1/4}$, the physiological mortality becomes $\alpha = c/A$

LIFE HISTORY OPTIMIZATION OF OFFSPRING SIZE

The optimal life history strategy in terms of offspring size and adult size is the strategy that maximizes lifetime reproductive output (Charnov 1993). In optimal life history theory, lifetime reproductive output is determined by the mortality and the available energy as functions of size or age. Here, we determine the offspring size that maximizes lifetime reproductive output using arguments from Christiansen & Fenchel (1979) and Andersen et al. (2008).

The available energy can be assumed from metabolic scaling arguments to be $H(w) = Aw^n$, where the usual metabolic assumption is $n = 3/4$ (West et al. 1997). Consumption results in a prey mortality of $\mu(w) = \alpha w^{n-1}$, where α is a dimensionless constant relating consumption and mortality (Andersen & Beyer 2006). For simplicity, we assume determinate growth where a juvenile uses all acquired energy for growth and a mature individual of size W uses all energy for reproduction; however, the central results are valid for indeterminate growth as well (Andersen et al. 2008). The lifetime reproductive output (expected number of offspring during life) is

$$R_0 = \frac{\epsilon}{2} P_{w_0 \rightarrow W} \frac{H(W)}{w_0 \mu(W)},$$

where ϵ is the reproductive efficiency, the division by 2 assumes an even sex ratio, $H(W)$ is the adult rate of reproduction (mass per unit time), $1/\mu(W)$ is the expected adult life span, $1/w_0$ is to convert from units of mass to number of offspring, and the probability of surviving from offspring size w_0 to adult size W is

$$P_{w_0 \rightarrow W} = \exp \left[- \int_{w_0}^W \frac{\mu(w)}{H(w)} dw \right].$$

Inserting the metabolic assumptions $H(w) = Aw^n$ and $\mu(w) = \alpha Aw^{n-1}$ yields a lifetime reproductive output of

$$R_0 = \frac{\epsilon}{2\alpha} \left(\frac{W}{w_0} \right)^{1-\alpha}.$$

Three conclusions can be drawn from this result:

1. If $R_0 < 1$, then each female produces less than a single offspring throughout life, yielding an unsustainable population.
2. Lifetime reproductive output depends only on the ratio between adult size and offspring size. The absolute values of the two sizes do not matter.
3. The larger the ratio between adult and offspring size, the higher the fitness. Organisms will therefore strive to maximize this ratio under the constraints of other external factors (Neuheimer et al. 2015).

Note that the arguments above ignore the maintenance metabolism and indeterminate growth to simplify the mathematical derivation, but both of these effects can be accounted for (Andersen et al. 2008).

Offspring Size Strategies

Observed offspring size strategies employed by marine life can be roughly partitioned into two groups: a fixed-ratio strategy in which offspring size is a constant fraction of adult size, and a small-eggs strategy in which offspring size is invariant, i.e., independent of adult size (Neuheimer et al. 2015) (**Figure 7**). Crustaceans, cartilaginous fish, and cetaceans employ the fixed-ratio strategy, with an adult:offspring weight ratio of approximately 100:1. The metabolic optimal life history theory (Equation 7) is unable to predict the fixed-ratio strategy. For marine mammals, the fixed-ratio strategy can be explained by the need to perform parental care; it simply becomes increasingly difficult for a parent to provide care when the offspring is much smaller than the parent (Shine

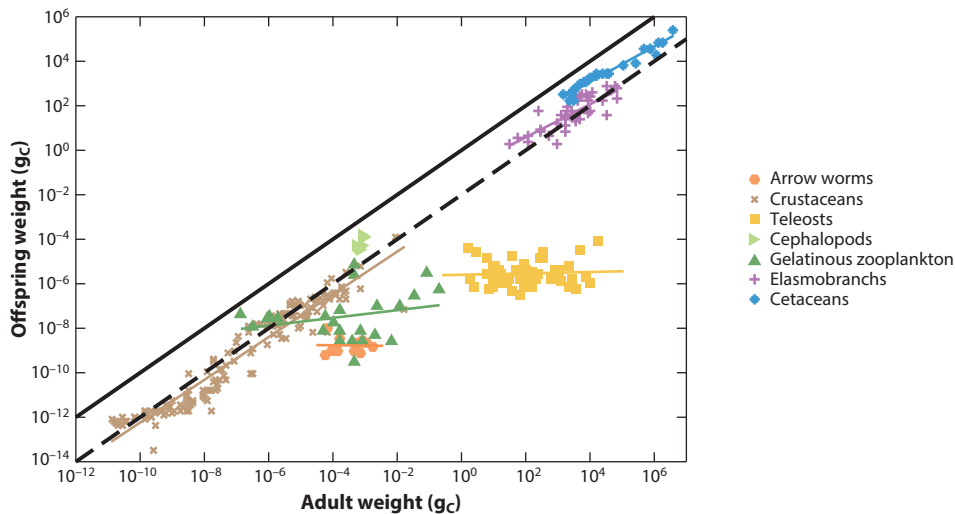



Figure 7

Weights of adults and offspring for metazoans grouped by species of similar taxonomy. Estimates of mean adult and offspring sizes were compiled from the literature, with adults defined as individuals that had reached maturity and offspring defined as the smallest size at which offspring are independent of the parent (see **Supplemental Tables 6** and **7**). The original data included measures of volume, length, wet weight, dry weight, and carbon dry weight, all of which were converted to carbon dry weight; this conversion used species-specific conversion factors when available, and group-specific conversion factors otherwise. The solid line is a 1:1 adult:offspring size ratio, and the dashed line is a 100:1 adult:offspring size ratio. Life forms along this line [cetaceans (*blue*), elasmobranchs (*purple*), and crustaceans (*brown*)] follow the fixed-ratio strategy, whereas life forms with invariant offspring size [most notably teleosts (*yellow*)] follow the small-eggs strategy.

 Supplemental Material

1978). For the other groups, the fixed-ratio strategy can be explained by an elaboration of the evolutionary argument in the second sidebar (Life History Optimization of Offspring Size) to account for density-dependent effects (K. Olsson, H. Gislason & K.H. Andersen, manuscript submitted). Such elaboration shows that the strategy that maximizes W/w_0 is optimal only if the offspring do not experience density-dependent effects at the time of hatching. If they do experience density-dependent survival early in life, an evolutionary stable strategy with $W/w_0 \approx 100$ emerges.

TRANSITIONS BETWEEN LIFE FORMS

We have reviewed how size influences resource acquisition, mobility, ability to sense prey, and life history strategy based on theoretical arguments and cross-species empirical analyses. We now use these relations to understand the mechanisms behind the transitions between the seven realms of marine life: molecular life (viruses), osmo-heterotrophic bacteria, unicellular phototrophs, unicellular mixotrophs and heterotrophs, planktonic multicellular heterotrophs with ontogenetic growth, visually foraging poikilotherms, and homeotherms (**Figure 1**, **Table 1**). These seven realms correspond to the traditional taxonomic division of life into viruses, bacteria, phytoplankton, uni- and multicellular zooplankton, fish, and marine mammals. Our alternative naming reflects the function of the groups and highlights the factors that determine the characteristic sizes where there is a transition between the groups.

A central theme is that the development of larger size opens up new possibilities for resource acquisition and sensing. Examples include how the battery of available senses increases with size (**Figure 6**), how the emergence of multicellularity makes it possible to increase the adult:offspring size ratio and thereby increase fitness (see sidebar Life History Optimization of Offspring Size), and how mortality decreases with size. Larger size therefore increases the competitive edge, provides access to new resources, and increases survival. This, of course, only works until the niche related to the larger size is filled, but it explains the evolutionary drive toward larger body size. The sizes where new possibilities appear often mark a transition between the major life forms because the utilization of new senses and other changes require fundamental alterations in body plan and life strategy.

From Viruses to Cells

The smallest size of a cell is approximately 10^{-15} g_C, with a diameter of approximately 0.1–1 μm. Organisms this small are believed to be functionally limited by metabolic constraints (Kempes et al. 2012) and the size of nonscalable components: genome size (DeLong et al. 2010) and in particular the cell wall (Raven 1994). The cell wall size alone can be used to calculate a lower limit for cell size: The wall has a mass $c_{\text{wall}}d^2$ and the cell itself has a mass cd^3 , where c_{wall} and c are constants. If we ignore the genome, a theoretical lower limit to cell size is where all cell mass is used by the wall:

$$d_{\text{limit}} = \frac{c_{\text{wall}}}{c}. \quad (8)$$

For a 0.5-μm cell, the wall comprises approximately 30% of the total mass (Raven 1994), so $c_{\text{wall}}/c \approx 0.3 \times 0.5$ μm. This gives a lower limit on cell size of $d_{\text{limit}} \approx 0.15$ μm.

From Osmo-Heterotrophs to Phototrophs

The smallest unicellular organisms are heterotrophic bacteria feeding on dissolved organic matter encountered through diffusion. At a diameter $(C_{\text{DOM}}b_{\text{D}})/(C_{\text{L}}b_{\text{L}})$ (Equation 4), it becomes favorable to fix inorganic carbon through photosynthesis instead of relying on dissolved organic matter. This size depends on the relative concentrations of dissolved organic matter (C_{DOM}) and light (C_{L}), but it can be as small as 10^{-14} g_C in the upper photic zone with very low concentrations of dissolved organic matter ($C_{\text{DOM}} \approx 5$ μg_C/L) and abundant light [$C_{\text{L}} \approx 7$ J/(day·m²)] and increases as light decreases (**Figure 4**).

From Phototrophs to Heterotrophs

The smallest phototrophs are expected to be carbon limited (which in practice means that they are limited by the amount of light, because dissolved inorganic carbon is assumed to be plentiful), whereas the largest phototrophs are expected to be nutrient limited. This difference emerges from the different scaling of nutrient encounter (which scales as l^1) and light encounter (which scales as l^2) (Equations 2 and 3, **Figure 3**). As before, the exact sizes where the transitions between light-limited phototrophs, nutrient-limited phototrophs, and heterotrophs occur depend on the specific conditions of dissolved nutrients, light, and suitable prey (**Figure 4b**). An order-of-magnitude estimate of the characteristic transition between phototrophs and pure heterotrophs is 10^{-7} g_C ($l \approx 6 \times 10^{-2}$ cm), but it can vary from 10^{-8} g_C in conditions with low light and high nutrients to 10^{-5} g_C in conditions with high light.

The size that marks the transition between phototrophs and heterotrophs is blurred by a large group of mixotrophic organisms that acquire nutrients and carbon for biomass synthesis through phagotrophy, while photosynthesis provides carbon primarily for metabolism. The mixotrophic strategy is most favorable for organisms with sizes in the transition between phototrophy and heterotrophy. The size range where the mixotrophic strategy is favorable varies with environmental conditions: It is vanishingly small in eutrophic conditions and increases to more than a factor of 10 in diameter in oligotrophic conditions, in agreement with observations (Barton et al. 2013).

Phagotrophy: taking up carbon and nutrients by absorbing other living organisms

Unicellular to Multicellular Life

The drive to develop larger size eventually leads to multicellular organisms. Multicellularity opens the possibility of specialized tissue for, e.g., sensory organs. Among microscopic metazoans, the dominant group of copepods has developed sensory apparatus to detect prey via hydromechanical cues and appendages to generate feeding currents and make jumps to escape predators. We have not developed a specific argument for the size where the transition to multicellularity occurs, but because life history theory predicts that increasing the adult:offspring size ratio increases lifetime reproductive output (Equation 7), it is likely to occur at the smallest possible size. DeLong et al. (2010) argued that this point is approximately $10^{-6} g_C$ ($\approx 1 \mu m$), the size at which it becomes possible to develop a fractal delivery network.

The life history argument in Equation 7 shows how metabolic constraints create an evolutionary drive to minimize offspring size and maximize adult size. This means that organisms within each metazoan group strive to extend their size range, but they are able to do so only within the limits defined by the sizes where there is a breakdown in a scaling relationship describing a vital function.

From Copepods to Fish

Fishes (including, from a functional perspective, cephalopods) are the dominant organisms in the size range from $1 mg_{WW}$ to approximately $100 kg_{WW}$ (1 cm to 2 m). Fish are characterized by being streamlined, visual predators. At sizes smaller than $1 mg_{WW}$, the dominating organisms are blind copepods, which have a very nonstreamlined body plan. The transition size between these two very different life forms is characterized by transitions between superior sensing modes (from mechanosensing to vision) and between hydromechanical regimes (from viscous to inertial). The change in hydromechanical regime explains the slender fish shape, but it also entails a change in feeding mode. Fish larvae employ suction feeding, which becomes increasingly difficult the smaller they are (China & Holzman 2014). Probably the most important transition is in sensing, with the lower size limit of fish coinciding with the lower size of a functioning eye. Were fish to make smaller eggs, their larvae would be unable to compete with the tactile-sensing copepods, which have a morphology designed for optimal movement and prey capture in a viscous fluid environment; were copepods to become larger, they would be outcompeted by visually sensing fish with streamlined bodies.

From Fish to Cetaceans

Cetaceans are the largest organisms in the oceans, occupying the size range from approximately $100 kg_{WW}$ and up. It is tempting to attribute the transition from fish to cetaceans to the appearance of echolocation as a possible sensing mode. However, only toothed cetaceans employ echolocation for sensing; baleen whales rely on the same senses as fish. If there are no changes in the power-law relationships determining sensing and food encounter, then why have teleosts not evolved even

larger sizes than the few hundred kilograms of the largest fish (bluefin tuna and sunfish, which have maximum weights of 450 and 1,000 kg_{WW}, respectively)? We propose two arguments for the transition between fish and cetaceans: a metabolically based upper limit of a water-breathing organism (Freedman & Noakes 2002, supplement to Makarieva et al. 2004) and a lower size limit of a homeothermic (warm-blooded) organism.

We have focused on resource acquisition in terms of carbon and nutrients, but heterotrophs also need oxygen to fuel their metabolism. The absorption of oxygen through gills is limited by the surface area of the gills. Because the surfaces of gills are fractal, they scale with an exponent between 2/3 and 1, probably very close to the metabolic exponent of 3/4. The acquisition of oxygen therefore scales with a similar exponent as metabolism, so the relative ability to acquire food and oxygen is independent of size. However, larger organisms accumulate heat created by activity and use this to elevate their metabolism. Notable examples are scombroids (tuna and marlin) and pelagic sharks (Block 1991). A high body temperature means higher activity and therefore higher predatory success against slower heterothermic (cold-blooded) prey. Such an increase in metabolism will eventually require more oxygen than can be obtained by pumping water over the gills. This problem is solved by ram ventilation, which provides a higher flow of water around the gills and therefore a higher oxygen absorption rate. Evidence for this is provided by the largest fish being either very active ram-ventilating fish (large scombroids and sharks) or relatively sluggish pumping fish (sunfish). We conjecture that it would be impossible for fish to develop homeothermy as a means of competing with cetaceans; the solubility of oxygen in water is simply too low to fuel a homeothermic metabolism. Cetaceans fuel their high homeothermic metabolism by breathing air, which has a much higher solubility of oxygen than water does.

For homeotherms, the loss of body heat should be included in the energy budget, as this defines a lower limit for the size of a homeotherm (Haldane 1928). Heat loss is a surface process that scales as $\propto \kappa w^{2/3}$, where κ is the thermal conductivity of water. Because organisms wish to minimize heat loss, their surface is not fractal and the exponent is not larger than 2/3. The energy for heating comes from the acquisition of resources (oxygen and food), which scales metabolically as $Aw^{3/4}$. The size where there is a balance between heat loss and resource acquisition defines a lower limit of homeothermy as $(A/\kappa)^{12}$ (Andersen et al. 2008). This lower limit is highly sensitive to the values of the parameters A and κ because their ratio is raised to a high exponent. For example, the ratio between the lower limits calculated for a marine and a terrestrial habitat is the ratio between the heat conductivity in air and water (≈ 20) raised to power 12, which gives 4×10^{15} . This factor is much larger than the ratio between the smallest cetacean, a harbor porpoise calf of approximately 10 kg, and the smallest terrestrial homeotherm, an Etruscan shrew (*Suncus etruscus*) of approximately 0.1 g. Nevertheless, it seems evident that the smallest land animals are limited by loss of heat (e.g., shrews huddle together to conserve heat), so how can cetaceans manage to attain a small size in the face of a larger heat loss? We hypothesize that they do so by having an insulating layer of blubber. To achieve a lower size of 10 kg (a factor of 10^6 smaller than predicted), cetaceans need to decrease heat losses by a factor of $10^{6/12} \approx 3.2$ relative to terrestrial animals, which is not out of scope.

BEYOND SIZE

We posit that individual size is the most important trait characterizing a pelagic organism. Knowing the size of an organism makes it possible to estimate, often within an order of magnitude, its metabolic rate, clearance rate, swimming speed, and sensory range. We have shown how that information facilitates inference of trophic strategy, sensory mode, body shape, and, to some degree, reproductive strategy. Although important, we have largely ignored the subtle interplay

between temperature, oxygen concentration, and size (Verberk & Atkinson 2013). Our exploration has concentrated on how an individual's physiology and interactions with the surrounding physical and biotic environment are constrained by body size. Because body size also plays a large role in predator-prey interactions (Barnes et al. 2008), it is central in constraining biomass distributions (Boudreau & Dickie 1992, Sheldon & Prakash 1972), food web topology (Petchey et al. 2008), and species diversity (Fenchel & Finlay 2004, May 1975, Reuman et al. 2014), all of which lie beyond our work here but highlight the central role of body size. Even though size can be characterized as a "master trait" (Litchman & Klausmeier 2008), it is not the only trait that characterizes an organism. The relevant question is then which other traits best characterize the variation around the mean in the reviewed relations with size (**Figures 2, 5, and 7**). We propose three candidate traits to consider: predator:prey size ratio, feeding mode for heterotrophic metazoans, and jellyness.

Among heterotrophic metazoans, there appear to be two dominant strategies for predator:prey size ratio: a strategy based on a fixed ratio in the range 10–100, which is followed by most fish and copepods (Barnes et al. 2008), and a strategy aimed at preying on organisms much smaller than the predator. The small-prey strategy is used by the largest zooplankton (pelagic tunicates) and the largest vertebrates (whale sharks and baleen whales). Organisms with a large predator:prey size ratio rely on filtering the water to catch the prey. It is presently unknown what drives the development of the two alternative, but apparently equally competitive, strategies.

The feeding mode determines whether an actively feeding predator encounters its prey through ambushing or cruising. It is often assumed that predation pressure is a function of size only and therefore independent of feeding strategy or sensing mode. This is not quite true. It is becoming increasingly evident that feeding strategy is associated with a trade-off in mortality: An ambush feeder will encounter fewer prey than a cruising predator, but it will also have less exposure to predation and therefore lower mortality. This is a special example of how behavior manipulates this trade-off between feeding gains and mortality (Lima & Dill 1990). A quantitative demonstration of this trade-off has been made for zooplankton based on laboratory experiments (Kjørboe 2013), and its importance for seasonal succession has been modeled (Mariani et al. 2013). These trade-offs likely apply at least qualitatively to other predators, e.g., fish.

A related trade-off is the development of a gelatinous body (jellyfish, box jellies, and pelagic tunicates). We argued above (see the section Size and Sensing) that visual predators would be superior to predators sensing their prey through hydromechanical forces. However, the inflated body size of gelatinous organisms results in a large encounter cross section and hence a higher clearance rate than that of nongelatinous organisms with the same carbon body mass. This is what makes the jelly strategy effective even in the same size range where visual predation is possible (Acuña et al. 2011), particularly under low-light conditions (Sørnes & Aksnes 2004). At the same time, the gelatinous body makes the organism less attractive to predators, thereby lowering its mortality. These two examples show how general rules of encounter, mobility, and sensing inferred from size scaling can be broken by other traits.

DISCLOSURE STATEMENT

The authors are not aware of any affiliations, memberships, funding, or financial holdings that might be perceived as affecting the objectivity of this review.

ACKNOWLEDGMENTS

K.H.A. thanks Mick Follows for hospitality at the Massachusetts Institute of Technology while the draft of this article was written. This work was supported by the Centre for Ocean Life, a

VKR Centre of Excellence supported by the Villum Foundation. Affiliations for authors of this article are as follows:

¹VKR Centre for Ocean Life and ²National Institute of Aquatic Resources, Technical University of Denmark, 2920 Charlottenlund, Denmark; email: kha@aqu.dtu.dk

³Marine Biological Section, University of Copenhagen, 3000 Helsingør, Denmark

⁴Consejo Nacional de Investigaciones Científicas y Técnicas, C1033AAJ Buenos Aires, Argentina

⁵Estación de Fotobiología Playa Unión, 9103 Rawson, Argentina

⁶Center for Macroecology, Evolution, and Climate, Natural History Museum of Denmark, University of Copenhagen, 2100 Copenhagen, Denmark

⁷Systemic Conservation Biology, J.F. Blumenbach Institute of Zoology and Anthropology, University of Göttingen, 37073 Göttingen, Germany

⁸Centre for Ecology and Evolution in Microbial Model Systems (EEMiS), Linnaeus University, 391 82 Kalmar, Sweden

⁹Department of Biomedical Sciences, University of Copenhagen, 2200 Copenhagen, Denmark

¹⁰Department of Oceanography, University of Hawai'i at Mānoa, Honolulu, Hawaii 96822

¹¹GEOMAR Helmholtz Centre for Ocean Research Kiel, 24148 Kiel, Germany

¹²Department of Physics, Technical University of Denmark, 2800 Kongens Lyngby, Denmark

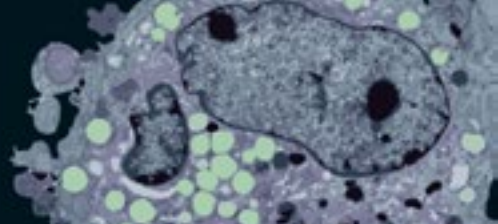
LITERATURE CITED

- Acuña JL, López-Urutia Á, Colin S. 2011. Faking giants: the evolution of high prey clearance rates in jellyfishes. *Science* 333:1627–29
- Aksnes D, Egge J. 1991. A theoretical model for nutrient uptake in phytoplankton. *Mar. Ecol. Prog. Ser.* 70:65–72
- Aksnes D, Utne A. 1997. A revised model of visual range in fish. *Sarsia* 82:137–47
- Andersen KH, Beyer JE. 2006. Asymptotic size determines species abundance in the marine size spectrum. *Am. Nat.* 168:54–61
- Andersen KH, Beyer JE, Pedersen M, Andersen NG, Gislason H. 2008. Life-history constraints on the success of the many small eggs reproductive strategy. *Theor. Popul. Biol.* 73:490–97
- Ara R, Amin SMN, Mazlan AG, Arshad A. 2013. Morphometric variation among six families of larval fishes in the Seagrass-Mangrove ecosystem of Gelang Patah, Johor, Malaysia. *Asian J. Anim. Vet. Adv.* 8:247–56
- Bagøien E, Kjørboe T. 2005. Blind dating—mate finding in planktonic copepods. I. Tracking the pheromone trail of *Centropages typicus*. *Mar. Ecol. Prog. Ser.* 300:105–15
- Barnes C, Bethea DM, Brodeur RD, Spitz J, Ridoux V, et al. 2008. Predator and prey body sizes in marine food webs. *Ecology* 89:881
- Barton AD, Finkel ZV, Ward BA, Johns DG, Follows MJ. 2013. On the roles of cell size and trophic strategy in North Atlantic diatom and dinoflagellate communities. *Limnol. Oceanogr.* 58:254–66
- Bejan A, Marden JH. 2006. Unifying constructal theory for scale effects in running, swimming and flying. *J. Exp. Biol.* 209:238–48
- Berg HC, Purcell EM. 1977. Physics of chemoreception. *Biophys. J.* 20:193–219
- Block BA. 1991. Evolutionary novelties: how fish have built a heater out of muscle. *Am. Zool.* 31:726–42
- Boudreau PR, Dickie LM. 1992. Biomass spectra of aquatic ecosystems in relation to fisheries yield. *Can. J. Fish. Aquat. Sci.* 49:1528–38
- Charnov EL. 1993. *Life History Invariants*. Oxford, UK: Oxford Univ. Press
- China V, Holzman R. 2014. Hydrodynamic starvation in first-feeding larval fishes. *PNAS* 111:8083–88
- Christiansen FB, Fenchel TM. 1979. Evolution of marine invertebrate reproductive patterns. *Theor. Popul. Biol.* 16:267–82
- Cohen J, Pimm S, Yodzis P, Saldaña J. 1993. Body sizes of animal predators and animal prey in food webs. *J. Anim. Ecol.* 62:67–78

- Collin SP, Whitehead D. 2004. The functional roles of passive electroreception in non-electric fishes. *Anim. Biol.* 54:1–25
- Curcio CA, Sloan KR, Kalina RE, Hendrickson AE. 1990. Human photoreceptor topography. *J. Comp. Neurol.* 292:497–523
- Davies-Colley RJ, Smith DG. 1995. Optically pure waters in Waikopu (“Pupu”) Springs, Nelson, New Zealand. *N.Z. J. Mar. Freshw. Res.* 29:251–56
- DeLong JP, Okie JG, Moses ME, Sibly RM, Brown JH. 2010. Shifts in metabolic scaling, production, and efficiency across major evolutionary transitions of life. *PNAS* 107:12941–45
- Dunbrack RL, Ware DM. 1987. Energy constraints and reproductive trade-offs determining body size in fishes. In *Evolutionary Physiological Ecology*, ed. P Calow, pp. 191–218. Cambridge, UK: Cambridge Univ. Press
- Dusenbery DB. 2009. *Living at Micro Scale: The Unexpected Physics of Being Small*. Cambridge, MA: Harvard Univ. Press
- Edwards KF, Thomas MK, Klausmeier CA, Litchman E. 2012. Allometric scaling and taxonomic variation in nutrient utilization traits and maximum growth rate of phytoplankton. *Limnol. Oceanogr.* 57:554–66
- Fenchel T. 1974. Intrinsic rate of natural increase: the relationship with body size. *Oecologia* 14:317–26
- Fenchel T. 1984. Suspended marine bacteria as a food source. In *Flows of Energy and Materials in Marine Ecosystems: Theory and Practice*, ed. MJR Fasham, pp. 301–15. NATO Conf. Ser. 11. New York: Plenum
- Fenchel T, Finlay BJ. 2004. The ubiquity of small species: patterns of local and global diversity. *BioScience* 54:777–84
- Fiksen Ø, Follows M, Aksnes D. 2013. Trait-based models of nutrient uptake in microbes extend the Michaelis-Menten framework. *Limnol. Oceanogr.* 58:193–202
- Finkel ZV. 2001. Light absorption and size scaling of light-limited metabolism in marine diatoms. *Limnol. Oceanogr.* 46:86–94
- Freedman JA, Noakes DLG. 2002. Why are there no really big bony fish? A point-of-view on maximum body size in teleosts and elasmobranchs. *Rev. Fish Biol. Fish.* 12:403–16
- Froese R, Pauly D. 2013. *FishBase*. <http://www.fishbase.org>
- Gillooly J, Charnov E, West G, Savage V, Brown J. 2002. Effects of size and temperature on developmental time. *Nature* 417:70–73
- Haldane JBS. 1928. On being the right size. In *A Treasury of Science*, ed. H Shapely, S Raffort, H Wright, pp. 321–25. New York: Harper
- Hansen BW, Bjørnsen PK, Hansen PJ. 1994. The size ratio between planktonic predators and their prey. *Limnol. Oceanogr.* 39:395–403
- Hansen PJ, Bjørnsen PK, Hansen BW. 1997. Zooplankton grazing and growth: scaling within the 2–2,000- μ m body size range. *Limnol. Oceanogr.* 42:687–704
- Hemmingsen AM. 1960. *Energy Metabolism as Related to Body Size and Respiratory Surfaces, and Its Evolution*. Rep. Steno Mem. Hosp. Nord. Insulinlab. Vol. 9, Pt. 2. Copenhagen, Den.: Niels Steensens Hosp.
- Hirst AG, Kiørboe T. 2002. Mortality of marine planktonic copepods: global rates and patterns. *Mar. Ecol. Prog. Ser.* 230:195–209
- Holling CS. 1959. Some characteristics of simple types of predation and parasitism. *Can. Entomol.* 91:385–98
- Hueter RE, Mann DA, Maruska KP, Sisneros JA, Demski LS. 2004. Sensory biology of elasmobranchs. In *Biology of Sharks and Their Relatives*, ed. JC Carrier, JA Musick, MR Heithaus, pp. 325–68. Boca Raton, FL: CRC
- Huntley ME, Zhou M. 2004. Influence of animals on turbulence in the sea. *Mar. Ecol. Prog. Ser.* 273:65–79
- Kempes CP, Dutkiewicz S, Follows MJ. 2012. Growth, metabolic partitioning, and the size of microorganisms. *PNAS* 109:495–500
- Kiørboe T. 1993. Turbulence, phytoplankton cell size, and the structure of pelagic food webs. *Adv. Mar. Biol.* 29:1–72
- Kiørboe T. 2001. Formation and fate of marine snow: small-scale processes with large-scale implications. *Sci. Mar.* 65(Suppl. 2):57–71
- Kiørboe T. 2011. How zooplankton feed: mechanisms, traits and trade-offs. *Biol. Rev. Camb. Philos. Soc.* 86:311–39

- Kjørboe T. 2013. Zooplankton body composition. *Limnol. Oceanogr.* 58:1843–50
- Kjørboe T, Andersen A, Langlois VJ, Jakobsen HH. 2010. Unsteady motion: escape jumps in planktonic copepods, their kinematics and energetics. *J. R. Soc. Interface* 7:1591–602
- Kjørboe T, Hirst AC. 2014. Shifts in mass-scaling of respiration, feeding, and growth rates across life-form transitions in marine pelagic organisms. *Am. Nat.* 183:E118–30
- Klausmeier C, Litchman E, Daufresne T, Levin S. 2004. Optimal nitrogen-to-phosphorus stoichiometry of phytoplankton. *Nature* 429:171–74
- Kleiber M. 1932. Body size and metabolism. *Hilgardia* 6:315–53
- Lima SL, Dill LM. 1990. Behavioral decisions made under the risk of predation: a review and prospectus. *Can. J. Zool.* 68:619–40
- Litchman E, Klausmeier CA. 2008. Trait-based community ecology of phytoplankton. *Annu. Rev. Ecol. Evol. Syst.* 39:615–39
- Litchman E, Klausmeier CA, Schofield OM, Falkowski PG. 2007. The role of functional traits and trade-offs in structuring phytoplankton communities: scaling from cellular to ecosystem level. *Ecol. Lett.* 10:1170–81
- Makarieva AM, Gorshkov VG, Bai-Lian L. 2004. Ontogenetic growth: models and theory. *Ecol. Model.* 176:15–26
- Marañón E, Cermeño P, López-Sandoval DC, Rodríguez-Ramos T, Sobrino C, et al. 2013. Unimodal size scaling of phytoplankton growth and the size dependence of nutrient uptake and use. *Ecol. Lett.* 16:371–79
- Mariani P, Andersen KH, Visser AW, Barton AD, Kjørboe T. 2013. Control of plankton seasonal succession by adaptive grazing. *Limnol. Oceanogr.* 58:173–84
- Martens EA, Wadhwa N, Jacobsen NS, Lindemann C, Andersen KH, Visser AW. 2015. Size structures sensory hierarchy in ocean life. *Proc. R. Soc. B* 282:20151346
- May RM. 1975. Patterns of species abundance and diversity. In *Ecology and Evolution of Communities*, ed. ML Cody, JL Diamond, pp. 81–120. Cambridge, MA: Belknap
- May RM, Godfrey J. 1994. Biological diversity: differences between land and sea. *Proc. R. Soc. B* 343:105–11
- Mei Z-P, Finkel ZV, Irwin AJ. 2009. Light and nutrient availability affect the size-scaling of growth in phytoplankton. *J. Theor. Biol.* 259:582–88
- Morel A, Bricaud A. 1981. Theoretical results concerning light absorption in a discrete medium, and application to specific absorption of phytoplankton. *Deep-Sea Res. A* 28:1375–93
- Morioka S, Vongvichith B, Phommachan P, Chantason P. 2013. Growth and morphological development of laboratory-reared larval and juvenile bighead catfish *Clarias macrocephalus* (Siluriformes: Clariidae). *Ichthyol. Res.* 60:16–25
- Moser HG, Sumida BY, Ambrose DA, Sandknop EM, Stevens EG. 1986. Development and distribution of larvae and pelagic juveniles of ocean whitefish, *Caulolatilus princeps*, in the CalCOFI survey region. *CalCOFI Rep.* 27:162–69
- Munk WH, Riley GA. 1952. Absorption of nutrients by aquatic plants. *J. Mar. Res.* 11:215–40
- Neuheimer AB, Hartvig M, Heuschele J, Hylander S, Kjørboe T, et al. 2015. Adult and offspring size in the ocean over 17 orders of magnitude follows two life-history strategies. *Ecology*. In press
- Northmore D, Volkman FC, Yager D. 1978. Vision in fishes: colour and pattern. In *The Behavior of Fish and Other Aquatic Animals*, ed. DI Mostofsky, pp. 79–136. San Diego, CA: Academic
- Oka S, Higashiji T. 2012. Early ontogeny of the big roughy *Gephyroberyx japonicus* (Beryciformes: Trachichthyidae) in captivity. *Ichthyol. Res.* 59:282–85
- Petchey OL, Beckerman AP, Riede JO, Warren PH. 2008. Size, foraging, and food web structure. *PNAS* 105:4191–96
- Peters RH. 1983. *The Ecological Implications of Body Size*. Cambridge, UK: Cambridge Univ. Press
- Peterson I, Wroblewski J. 1984. Mortality rate of fishes in the pelagic ecosystem. *Can. J. Fish. Aquat. Sci.* 41:1117–20
- Rall BC, Brose U, Hartvig M, Kalinkat G, Schwarzmüller F, et al. 2012. Universal temperature and body-mass scaling of feeding rates. *Philos. Trans. R. Soc. B* 367:2923–34
- Raven JA. 1994. Why are there no picoplanktonic O₂ evolvers with volumes less than 10⁻¹⁹ m³? *J. Plankton Res.* 16:565–80
- Reuman DC, Gislason H, Barnes C, Mélin F, Jennings S. 2014. The marine diversity spectrum. *J. Anim. Ecol.* 83:963–79

- Sambily VC Jr. 1990. Interrelationships between swimming speed, caudal fin aspect ratio and body length of fishes. *Fishbyte* 8:16–20
- Schwaderer AS, Yoshiyama K, de Tezanos Pinto P, Swenson NG, Klausmeier CA, Litchman E. 2011. Eco-evolutionary differences in light utilization traits and distributions of freshwater phytoplankton. *Limnol. Oceanogr.* 56:589–98
- Sheldon RW, Prakash A. 1972. The size distribution of particles in the ocean. *Limnol. Oceanogr.* 17:327–40
- Sheldon RW, Sutcliffe WH Jr, Paranajpe MA. 1977. Structure of pelagic food chain and relationship between plankton and fish production. *J. Fish. Res. Board Can.* 34:2344–53
- Shine R. 1978. Propagule size and parental care: the “safe harbor” hypothesis. *J. Theor. Biol.* 75:417–24
- Sørnes TA, Aksnes DL. 2004. Predation efficiency in visual and tactile zooplanktivores. *Limnol. Oceanogr.* 49:69–75
- Stoecker DK. 1998. Conceptual models of mixotrophy in planktonic protists and some ecological and evolutionary implications. *Eur. J. Protistol.* 34:281–90
- Taguchi S. 1976. Relationship between photosynthesis and cell size of marine diatoms. *J. Phycol.* 12:185–89
- Tambi H, Flaten G, Egge J, Bødtker G, Jacobsen A, Thingstad TF. 2009. Relationship between phosphate affinities and cell size and shape in various bacteria and phytoplankton. *Aquat. Microb. Ecol.* 57:311–20
- Tennekes H, Lumley JL. 1972. *A First Course in Turbulence*. Cambridge, MA: MIT Press
- Thronsen J, Hasle G, Tangen K. 2003. *Norsk Kystplanktonflora*. Oslo, Nor.: Almatier
- Tomas CR. 1997. *Identifying Marine Phytoplankton*. San Diego, CA: Academic
- Verberk WCEP, Atkinson D. 2013. Why polar gigantism and Palaeozoic gigantism are not equivalent: effects of oxygen and temperature on the body size of ectotherms. *Funct. Ecol.* 27:1275–85
- Visser AW. 2001. Hydromechanical signals in the plankton. *Mar. Ecol. Prog. Ser.* 222:1–24
- Visser AW, Jackson GA. 2004. Characteristics of the chemical plume behind a sinking particle in a turbulent water column. *Mar. Ecol. Prog. Ser.* 283:55–71
- Ware DM. 1978. Bioenergetics of pelagic fish: theoretical change in swimming speed and ration with body size. *J. Fish. Res. Board Can.* 35:220–28
- Watkins JL, Brierley AS. 2002. Verification of the acoustic techniques used to identify Antarctic krill. *ICES J. Mar. Sci.* 59:1326–36
- Webb P. 1988. Simple physical principles and vertebrate aquatic locomotion. *Am. Zool.* 28:709–25
- West GB, Brown JH, Enquist BJ. 1997. A general model for the origin of allometric scaling laws in biology. *Science* 276:122–26
- Winberg GG. 1960. *Rate of Metabolism and Food Requirements of Fishes*. Fish. Res. Board Can. Transl. Ser. 194. Nanaimo, BC: Fish. Res. Board Can. Biol. Stn.



New From Annual Reviews:

Annual Review of Cancer Biology

cancerbio.annualreviews.org • Volume 1 • March 2017

ONLINE NOW!

Co-Editors: **Tyler Jacks**, *Massachusetts Institute of Technology*

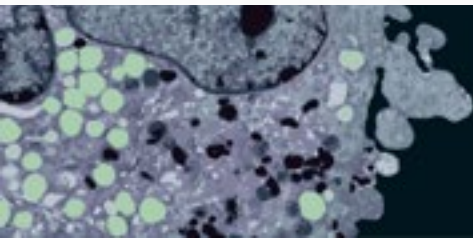
Charles L. Sawyers, *Memorial Sloan Kettering Cancer Center*

The *Annual Review of Cancer Biology* reviews a range of subjects representing important and emerging areas in the field of cancer research. The *Annual Review of Cancer Biology* includes three broad themes: Cancer Cell Biology, Tumorigenesis and Cancer Progression, and Translational Cancer Science.

TABLE OF CONTENTS FOR VOLUME 1:

- *How Tumor Virology Evolved into Cancer Biology and Transformed Oncology*, Harold Varmus 
- *The Role of Autophagy in Cancer*, Naiara Santana-Codina, Joseph D. Mancias, Alec C. Kimmelman
- *Cell Cycle-Targeted Cancer Therapies*, Charles J. Sherr, Jiri Bartek
- *Ubiquitin in Cell-Cycle Regulation and Dysregulation in Cancer*, Natalie A. Borg, Vishva M. Dixit
- *The Two Faces of Reactive Oxygen Species in Cancer*, Colleen R. Reczek, Navdeep S. Chandel
- *Analyzing Tumor Metabolism In Vivo*, Brandon Faubert, Ralph J. DeBerardinis
- *Stress-Induced Mutagenesis: Implications in Cancer and Drug Resistance*, Devon M. Fitzgerald, P.J. Hastings, Susan M. Rosenberg
- *Synthetic Lethality in Cancer Therapeutics*, Roderick L. Beijersbergen, Lodewyk F.A. Wessels, René Bernards
- *Noncoding RNAs in Cancer Development*, Chao-Po Lin, Lin He
- *p53: Multiple Facets of a Rubik's Cube*, Yun Zhang, Guillermina Lozano
- *Resisting Resistance*, Ivana Bozic, Martin A. Nowak
- *Deciphering Genetic Intratumor Heterogeneity and Its Impact on Cancer Evolution*, Rachel Rosenthal, Nicholas McGranahan, Javier Herrero, Charles Swanton
- *Immune-Suppressing Cellular Elements of the Tumor Microenvironment*, Douglas T. Fearon
- *Overcoming On-Target Resistance to Tyrosine Kinase Inhibitors in Lung Cancer*, Ibiayi Dagogo-Jack, Jeffrey A. Engelman, Alice T. Shaw
- *Apoptosis and Cancer*, Anthony Letai
- *Chemical Carcinogenesis Models of Cancer: Back to the Future*, Melissa Q. McCreery, Allan Balmain
- *Extracellular Matrix Remodeling and Stiffening Modulate Tumor Phenotype and Treatment Response*, Jennifer L. Leight, Allison P. Drain, Valerie M. Weaver
- *Aneuploidy in Cancer: Seq-ing Answers to Old Questions*, Kristin A. Knouse, Teresa Davoli, Stephen J. Elledge, Angelika Amon
- *The Role of Chromatin-Associated Proteins in Cancer*, Kristian Helin, Saverio Minucci
- *Targeted Differentiation Therapy with Mutant IDH Inhibitors: Early Experiences and Parallels with Other Differentiation Agents*, Eytan Stein, Katharine Yen
- *Determinants of Organotropic Metastasis*, Heath A. Smith, Yibin Kang
- *Multiple Roles for the MLL/COMPASS Family in the Epigenetic Regulation of Gene Expression and in Cancer*, Joshua J. Meeks, Ali Shilatifard
- *Chimeric Antigen Receptors: A Paradigm Shift in Immunotherapy*, Michel Sadelain

Annu. Rev. Mar. Sci. 2016.8:217-241. Downloaded from www.annualreviews.org. Access provided by 108.28.245.38 on 07/06/17. For personal use only.





Contents

Global Ocean Integrals and Means, with Trend Implications <i>Carl Wunsch</i>	1
Visualizing and Quantifying Oceanic Motion <i>T. Rossby</i>	35
Cross-Shelf Exchange <i>K.H. Brink</i>	59
Effects of Southern Hemisphere Wind Changes on the Meridional Overturning Circulation in Ocean Models <i>Peter R. Gent</i>	79
Near-Inertial Internal Gravity Waves in the Ocean <i>Matthew H. Alford, Jennifer A. MacKinnon, Harper L. Simmons, and Jonathan D. Nash</i>	95
Mechanisms of Physical-Biological-Biogeochemical Interaction at the Oceanic Mesoscale <i>Dennis J. McGillicuddy Jr.</i>	125
The Impact of Submesoscale Physics on Primary Productivity of Plankton <i>Amala Mahadevan</i>	161
Changes in Ocean Heat, Carbon Content, and Ventilation: A Review of the First Decade of GO-SHIP Global Repeat Hydrography <i>L.D. Talley, R.A. Feely, B.M. Sloyan, R. Wanninkhof, M.O. Baringer, J.L. Bullister, C.A. Carlson, S.C. Doney, R.A. Fine, E. Firing, N. Gruber, D.A. Hansell, M. Ishii, G.C. Johnson, K. Katsumata, R.M. Key, M. Kramp, C. Langdon, A.M. Macdonald, J.T. Mathis, E.L. McDonagh, S. Mecking, F.J. Millero, C.W. Mordy, T. Nakano, C.L. Sabine, W.M. Smethie, J.H. Swift, T. Tanhua, A.M. Thurnherr, M.J. Warner, and J.-Z. Zhang</i>	185
Characteristic Sizes of Life in the Oceans, from Bacteria to Whales <i>K.H. Andersen, T. Berge, R.J. Gonçalves, M. Hartvig, J. Heuschele, S. Hylander, N.S. Jacobsen, C. Lindemann, E.A. Martens, A.B. Neubeimer, K. Olsson, A. Palacz, A.E.F. Prowe, J. Sainmont, S.J. Traving, A.W. Visser, N. Wadhwa, and T. Kjørboe</i>	217

Mangrove Sedimentation and Response to Relative Sea-Level Rise <i>C.D. Woodroffe, K. Rogers, K.L. McKee, C.E. Lovelock, I.A. Mendelsohn, and N. Saintilan</i>	243
The Great <i>Diadema antillarum</i> Die-Off: 30 Years Later <i>H.A. Lessios</i>	267
Growth Rates of Microbes in the Oceans <i>David L. Kirchman</i>	285
Slow Microbial Life in the Seabed <i>Bo Barker Jørgensen and Ian P.G. Marshall</i>	311
The Thermodynamics of Marine Biogeochemical Cycles: Lotka Revisited <i>Joseph J. Vallino and Christopher K. Algar</i>	333
Multiple Stressors in a Changing World: The Need for an Improved Perspective on Physiological Responses to the Dynamic Marine Environment <i>Alex R. Gunderson, Eric J. Armstrong, and Jonathon H. Stillman</i>	357
Nitrogen and Oxygen Isotopic Studies of the Marine Nitrogen Cycle <i>Karen L. Casciotti</i>	379
Sources, Ages, and Alteration of Organic Matter in Estuaries <i>Elizabeth A. Canuel and Amber K. Hardison</i>	409
New Approaches to Marine Conservation Through the Scaling Up of Ecological Data <i>Graham J. Edgar, Amanda E. Bates, Tomas J. Bird, Alun H. Jones, Stuart Kininmonth, Rick D. Stuart-Smith, and Thomas J. Webb</i>	435
Ecological Insights from Pelagic Habitats Acquired Using Active Acoustic Techniques <i>Kelly J. Benoit-Bird and Gareth L. Lawson</i>	463
Ocean Data Assimilation in Support of Climate Applications: Status and Perspectives <i>D. Stammer, M. Balmaseda, P. Heimbach, A. Köhl, and A. Weaver</i>	491
Ocean Research Enabled by Underwater Gliders <i>Daniel L. Rudnick</i>	519

Errata

An online log of corrections to *Annual Review of Marine Science* articles may be found at <http://www.annualreviews.org/errata/marine>